A steady-state simulation methodology for predicting runaway speed in Francis turbines

H. Hosseinimanesh[1], T. C. Vu[2], C. Devals[3], B. Nennemann[2] and F. Guibault[3]

[1]Department of Mechanical Engineering, École Polytechnique de Montréal, Montréal, Québec, Canada [2]Andritz-Hydro Ltd. Pointe-Claire, Québec, Canada, [3]Department of Computer and Software Engineering, École Polytechnique de Montréal, Montréal, Québec, Canada,

hossein.hosseinimanesh@polymtl.ca

Abstract. Runaway speed is an important performance factor for the safe operation of hydropower systems. In turbine design, the manufacturers must conduct several model tests to calculate the accurate value of runaway speed for the complete range of operating conditions, which are expensive and time-consuming. To study runaway conditions, the application of numerical tools such as unsteady CFD simulations can help to better understand the complex flow physics during transient processes. However, unsteady simulations require significant computational effort to compute accurate values of runaway speed due to difficulties related to unsteady turbulent flow modelling and instabilities. The present study presents a robust methodology based on steady-state RANS flow simulations capable of predicting the runaway speed of a Francis turbine with an adequate level of accuracy and in a reasonable simulation time. The simulations are implemented using a commercial flow solver and an iterative algorithm that relies on a smooth relation between turbine torque and speed coefficient. The impact of friction has been considered when estimating turbine torque, in order to improve the accuracy. The results of this study show good agreement with experiments.

1. Introduction

Hydropower manufacturers must guarantee the performance of the turbine runner at the end of the design process. Hence tests are performed on homologous models to demonstrate the guaranteed values of dynamic parameters such as the efficiency, cavitation, stability, runaway, and hydraulic axial thrust for the complete range of operating conditions. Among these parameters, runaway speed has an essential role in ensuring the safety of a power plant.

Runaway speed is the maximum speed attained during no-load operation of a turbine-generator with wicket gates fully open at maximum head. It happens when the control system fails to close rapidly the vanes during a load rejection event, and this failure may lead to dangerous situations. The runner speed continues to rise while there is no generator-load to dissipate the runner kinetic energy. Under such circumstances, slim structures such as turbine blades may be deformed due to increased centrifugal and hydraulic forces. Consequently, the rotor may become unbalanced and produce vibration, which can lead to failure of the entire turbine. Although the runaway speed occurs far from the turbine design operating condition, it is a plausible event during an emergency situation such as a fault of the control system during emergency shutdown. Thus the accurate prediction of runaway


Content from this work may be used under the terms of the Creative Commons Attribution 3.0 licence. Any further distribution of this work must maintain attribution to the author(s) and the title of the work, journal citation and DOI.
Published under licence by IOP Publishing Ltd

speed at different wicket gate angles is necessary to ensure the structural integrity of turbine components and the safety of the hydropower plant.

An accurate value of runaway speed is usually obtained from model tests, which are performed by the turbine manufacturers. Experimental tests are expensive and time-consuming. Thus it is desirable to develop alternative numerical methods for computing runaway speed of prototype turbines. For this purpose, hydro acoustic models are fast and robust, and allow simulating the dynamic behavior of the complete hydropower plant. Nicolet [1] used a 1D hydro acoustic method for modeling the hydraulic components of a hydropower plant in both transient and steady modes. The model could show the evolution of turbine dynamic parameters such as rotational speed, pressure and discharge during a load rejection event. However, this method depends on experimental data. For instance it required the turbine hill-chart to determine its corresponding hydraulic resistance and inductance in transient simulations.

Over the past two decades, industrial computational fluid dynamics (CFD) has been applied for solving difficult engineering problems because of computational capacity increase and numerical techniques advancements. In hydro turbines, unsteady CFD simulations have been used for analyzing highly turbulent flows at off-design conditions. The results showed the existence of unsteady flow phenomena such as vortex break down, rotor-stator interaction and vortex shedding inside flow passages [2-5]. Furthermore unsteady simulations were used for simulating transient processes which are the most damaging events for hydro turbines. Cherny [6] applied a 3D unsteady incompressible fluid model for studying the evolution of vortex structures and their effect during transient processes in Francis turbines. Kolšek [7] predicted the rotational speed, axial force and pressure at selected points during the shut-down of an axial water turbine. Nicolle [8] obtained the loading on the blades in a 3D transient numerical simulation of a hydraulic turbine during the start-up phase.

The flow structure in the hydro turbines is highly complex. Hence reaching an adequate level of precision in unsteady CFD simulations depends on the use of very fine meshes, small time steps and complex turbulence models, which require enormous computing resources and large simulation times. Consequently, the unsteady CFD approaches would not be fast and robust enough for calculating global performance characteristics of hydro turbines in design mode. In contrast, the steady CFD is now able to predict hydro turbine characteristics in shorter computational time with adequate level of accuracy and less computational resources. Vu [9] used steady-state stage computations for accurate prediction of efficiency characteristics of a Francis turbine near its best efficiency point. He also showed steady-state simulations to be a highly effective methodology for comparing global draft tube performance for nearby design operating points [10]. However, to the authors knowledge, the capacity of steady state RANS to accurately assess turbine runaway speed over a range of operating conditions has not been evaluated.

This paper presents a robust methodology based on steady-state RANS flow simulations in order to compute the runaway speed of a Francis turbine with an adequate level of accuracy and in a reasonable simulation time. The simulations are implemented using the commercial flow solver Ansys CFX and an iterative algorithm that relies on the smooth relation between turbine torque and speed factor. The impact of friction has been considered when estimating turbine torque, in order to improve the accuracy.

2. Computational aspect

The numerical study is performed on three test cases that include high and medium head Francis turbines in order to evaluate the capability of the proposed methodology to estimate runaway speed for a range of machines. The numerical results are validated using data obtained during model test measurements by Andritz Hydro.

2.1. Geometry and mesh description

The computational domain for all test cases encompasses a distributor channel (one stay vane, one guide vane), a runner passage (hub, shroud, blade) and the draft tube as can be seen in figure 1 for test

case 1. The summary of turbine characteristics is shown in table 1. Test cases 2 and 3 consist of the same geometries for all components except the runner blade.

Table 1. Test case specifications.

	Runner type
Case 1	Low head Francis turbine
Case 2	High head Francis turbine
Case 3	High head Francis turbine

The geometries and meshes of the components were generated using Andritz design tools. Multi-bloc-structured meshes for runner channel and draft tube, and hybrid meshes in a single domain for the guide vane and stay vane channels were used. For example, figure 2 shows the computational mesh for each component for test case 1. The complete computational domain of test cases 1, 2 and 3 comprised of 554k, 811k, and 813k mesh nodes respectively, as detailed in table 2.

Table 2. Number of nodes for simulation domains.

	Stay vane & guide vane	Runner blade	Draft tube	
Mesh type	Hexahedra and prisms	Hexahedra	Hexahedra	Total
Case 1	167k	144k	243k	554k
Case 2	170k	435k	206k	811k
Case 3	170k	437k	206k	813k

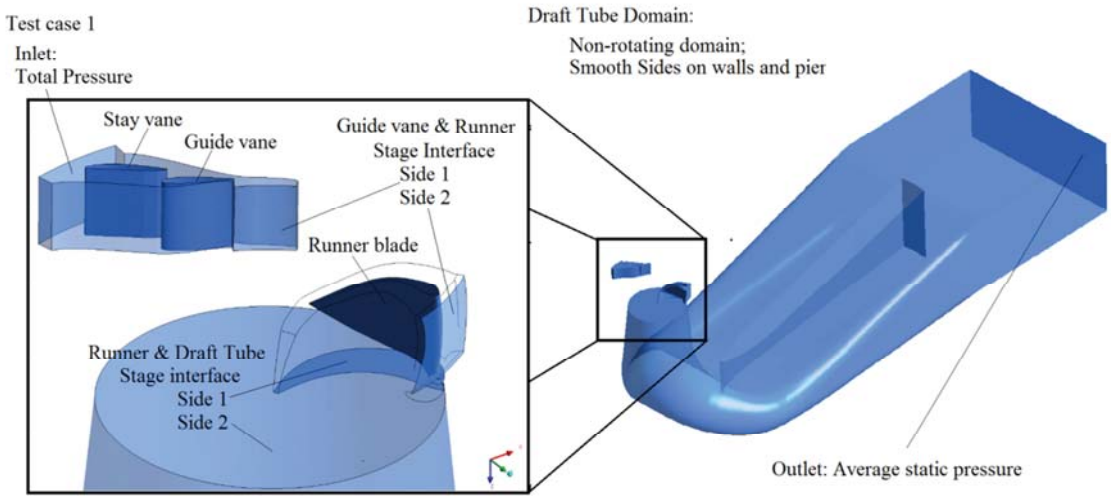

Figure 1. Geometry and boundary conditions of computational domains (test case 1).

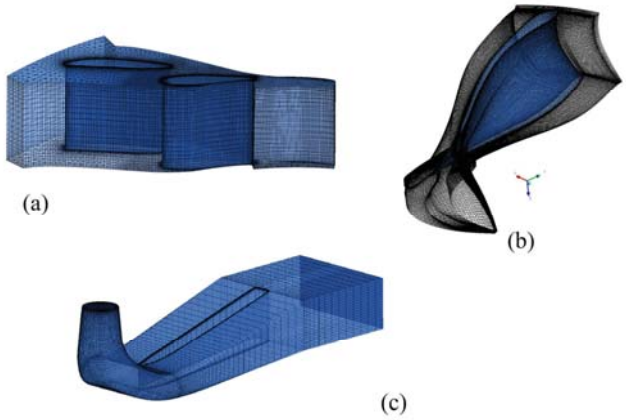

Figure 2. Mesh for components (test case 1).

2.2. Numerical set-up

In the present study, the runaway speed is calculated by performing steady Reynolds averaged Navier-Stokes 3D calculations at different operating conditions using Ansys-CFX 14 commercial solver. The Reynolds-averaged Navier-Stokes equations (RANS) are given by

$$\frac{\partial U_i}{\partial x_i} = 0 \tag{1}$$

$$\rho \frac{\partial U_i}{\partial t} + \rho \frac{\partial (U_j U_i)}{\partial x_j} = -\frac{\partial P}{\partial x_i} + f + \mu \left(\frac{\partial^2 U_i}{\partial x_j^2} \right) + \rho \frac{\partial}{\partial x_j} \overline{u_i' u_j'} \tag{2}$$

where U is the average velocity (m/s), ρ is the fluid density (kg/m^3), f is the body force of unit mass fluid (N), μ is the dynamic viscosity of water (N s/m^2), P is the average pressure (N/m^2), and $\rho \overline{u_i' u_j'}$ is the Reynolds shear stress (N/m^2), which can be written based on the Boussinesq hypothesis [11] as:

$$\rho \overline{u_i' u_j'} = -\mu_t \left(\frac{\partial u_i}{\partial x_j} + \frac{\partial u_j}{\partial x_i} \right) + \frac{2}{3} \rho \delta_{ij} k \tag{3}$$

where $k = \frac{1}{2} \sqrt{\overline{u_i' u_i'}}$ is the turbulent kinetic energy, and δ_{ij} is the Kronecker delta, μ_t is the turbulent viscosity.

The standard k-ε turbulence model is applied for treating turbulence. The standard k-ε model is known as a reliable and robust turbulence model for simulating high Reynolds number flows in Francis turbines. Galvan's [12] investigation on the steady state swirling flow in a draft tube showed that the standard k-ε turbulence model demonstrates good balance between reliable performance and computational cost.

The standard k-ε model is based on two transport equations, one for turbulent kinetic energy k, and the other for the turbulent dissipation ε. The transport equations for turbulent kinetic energy, k, and its dissipation rate, ε, are written as:

$$\frac{\partial \rho k}{\partial t} + \frac{\partial (\rho U_j k)}{\partial x_j} = \frac{\partial}{\partial x_j} \left[\left(\mu + \frac{\mu_t}{\sigma_k} \right) \frac{\partial k}{\partial x_j} \right] + P_k - \rho \varepsilon \tag{4}$$

$$P_k = \rho\overline{u_i' u_j'}\frac{\partial \rho U_i}{\partial x_j} \tag{5}$$

$$\frac{\partial \rho\varepsilon}{\partial t} + \frac{\partial(\rho U_j \varepsilon)}{\partial x_j} = \frac{\partial}{\partial x_j}\left[\left(\mu + \frac{\mu_t}{\sigma_\varepsilon}\right)\frac{\partial \varepsilon}{\partial x_j}\right] + C_{\varepsilon 1} P_k \frac{\varepsilon}{K} - \rho C_{\varepsilon 2}\frac{\varepsilon^2}{K}. \tag{6}$$

The standard *k-ε* model equations include the empirical constants σ_k=*1.0,* σ_ε=*1.3,*$C_{\varepsilon 1} = 1.44$, and $C_{\varepsilon 2}$=*1.92*.

The turbulent viscosity is expressed by:

$$\mu_t = \rho C_\mu \frac{k^2}{\varepsilon} \tag{7}$$

where C_μ =*0.09* is a constant number.

The momentum equations and turbulent advection equations have been discretized using the high-resolution scheme and first-order scheme respectively. Moreover, the convergence tolerances of all main primitive variables were set to 1×10^{-5} on the root mean square (RMS) residuals. Besides, the quantities of torque and inflow were tracked during simulation of monitoring points. Whenever their averaged values became steady, the solution was considered to have converged. The steady stage simulations were performed using one distributor channel as a stationary component and a runner blade passage as a rotating component in order to improve the computation cost. A stage interface was used for connecting the runner and distributor channel, and also the runner and draft tube modeled in distinct frames of reference. Radial runner blade passage interfaces were connected through fully matching rotational periodicity model. The scalable wall function was used, and mesh densities were chosen such that the mean value of y^+ remains in the range recommended by the flow solver. The inlet boundary condition was set to the total pressure associated to the turbine net head. The outlet boundary condition was specified as zero-averaged static pressure. No-slip boundary condition was imposed for all solid walls.

2.3. Turbine runaway speed computation methodology

The proposed methodology is based on the hypothesis that the turbine torque is a smooth function of the speed coefficient. In order to find runaway speed, we have to find the zero of the function. Algorithm 1 presents the proposed methodology for computing runaway speed. The first step consists in generating meshes from parametric geometry descriptions of each component. Then the numerical set-up is implemented as described in the previous section for the selected wicket gate angle. In step 3, we initialize the simulations for two operating point speed coefficients, $N_{ed,1}$ and $N_{ed,2}$ with best efficiency point speed value and 1.3 times of the same value, respectively. Then steady stage computations are performed for those points. In step 5 the blade torques T_1, T_2, and power coefficient $P_{ed,2}$ are derived from the converged simulations. Then we initialize the loop control value to 2 and start to compute the runaway speed in an iterative way as follows.

At the beginning, when $n = 2$, there are only two known points, namely $(N_{ed,1}, T_1)$ and $(N_{ed,2}, T_2)$. If the two points have the same sign for the torque, we use the secant method that passes a line through two points, and takes where it intersects abscissa as next point. Otherwise, we use the false position method. If $n > 2$, there are many known points $(N_{ed,1}, T_1), \dots, (N_{ed,n}, T_n)$, which lead to more available methods to estimate $N_{ed,n+1}$ such that T_{n+1} would be equal to zero. The simplest method is to use the last two points $(N_{ed,1}, T_1)$ and $(N_{ed,n}, T_n)$, and to compute $N_{ed,n+1}$ using again the secant method until two points of unlike torque sign are obtained. Afterward, the best choice is to use the false position method. This approach is proved to be efficient for calculating runaway speed.

In order to do fewer iterations of the main loop in algorithm 1, and to do fewer numerical simulations with Ansys CFX, some attempts were done to use more than the last two points, for example, by using a linear regression through the last three or four points or quadratic fitting of the last three points. This work is still in progress.

In algorithm 1, the process is considered to have converged, and $N_{ed,n}$ is considered as the runaway speed if one of the following conditions was satisfied.

- $\frac{|N_{ed,n+1} - N_{ed,n}|}{N_{ed,n}} < 2\ \%$ for two last points with different torque sign.
- The value of power coefficient $|P_{ed,n}|$ is less than 0.01.

Otherwise, we iterate, and compute the next operating condition, or stop if the loop control value n reaches the maximum value.

Algorithm 1 Computation of runaway speed.

Input: Wicket gate angle
Output: Runaway speed
1: Generate meshes
2: Numerical set-up
3: Initialize: Select speeds of two operating conditions $N_{ed,1}$, $N_{ed,2}$
4: Perform steady simulation for these two selected operating conditions
5: Compute torques T_1 , T_2, power coefficient $P_{ed,2}$ from steady simulation results
6: Set $n = 2$
7: **While** Simulation not converged **do** Steps 7.1-7.4
  7.1: From previous points $(N_{ed,n}, T_n)$, $(N_{ed,n-1}, T_{n-1}), \dots$, compute the next operating condition at $N_{ed,n+1}$
  7.2: Perform steady simulation at $N_{ed,n+1}$
  7.3: Derive torque $T_{n+1}$and power coefficient $P_{ed,n+1}$
  7.4: Set $n = n + 1$
8: $N_{ed,runaway\ speed} = N_{ed,n}$

In the runaway computation, the torque is calculated by

$$T = T_t(t) - T_{fr}(t) \tag{8}$$

where T_t, which is the turbine torque caused by pressure and viscous forces on the runner blade, is obtained from steady simulation results. The T_{fr} term, which is the friction torque on the crown and band of turbine, is opposing the driving torque during runaway transient. The friction torque is calculated as follows:

$$T_{fr} = T_{fr,crown} + T_{fr,band}. \tag{9}$$

The friction torques $T_{fr,crown}$ and $T_{fr,band}$ have an impact on the crown and band sections, respectively. The friction torque impact on the crown surface is estimated using a model that was established based on the approximation of a smooth rotating disk in a housing with turbulent flow[13]. The friction torque on the crown is estimated by

$$T_{fr,crown} = \frac{C_m \rho \omega^2 r_{crown}^5}{2} \tag{10}$$

where ω is the runner angular velocity (rad/sec), r_{crown} is the runner leading edge radius at the crown, ρ is the water density (kg/ m^3), and C_m is the torque coefficient, defined as

$$C_m = 0.0311 \left(\frac{1}{Re^{0.2}}\right)\left(\frac{r_{crown}}{GAP_C}\right)^{0.1} \tag{10}$$

where GAP_C is the width of the runner crown clearance (m), and *Re* is the Reynolds number, which is equal to

$$Re = \frac{\omega \rho r_{crown}^2}{\mu}. \quad (12)$$

In order to calculate the band torque, the band rotation was approximated by two concentric cylinders with the inner cylinder rotating with angular velocity ω, and the outer cylinder at rest. In the present work, Bilge's equation [14], which is an empirical relation of torque coefficient of coaxial cylinders, was applied for calculating the runner torque as follow:

$$T_{fr,band} = \frac{C_n \rho \pi \omega^2 \bar{r}_{band}^4 \cdot l_i}{2} \quad (13)$$

where l_i is the band seal length, and $\bar{r}_{band}$ is the average band radius. The moment coefficient for turbulent flow regimes with $Re > 10^4$ is defined as

$$C_n = 0.065\left(\frac{Gap}{\bar{r}_{band}}\right)^{0.3}(Re)^{-0.2} \quad (14)$$

where $Re = \frac{\rho \omega Gap \bar{r}_{band}}{\mu}$ is the Couette Reynolds number, Gap is the width of the runner band clearance, and $\bar{r}_{band}$ is the average radius of the band.

3. Results

The steady-state stage computations were performed on three test cases in order to assess the accuracy of the proposed methodology. For each test case, we numerically calculated the dynamic parameters at runaway: the speed coefficient N_{ed}, discharge coefficients Q_{ed} and power coefficient P_{ed}, defined by equations (15-17), for different opening angles.

$$N_{ed} = \frac{n\,D}{60\sqrt{gH}} \quad (15)$$

$$Q_{ed} = \frac{Q}{D^2\sqrt{gH}} \quad (16)$$

$$P_{ed} = \frac{2\pi T n}{60 g^{1.5} H^{1.5} \rho D^2} \quad (17)$$

where D is the runner reference diameter (m), g is the gravitational acceleration (m/s^2), H is the net head (m), n is the rotational speed (rpm), T is the shaft torque (Nm).

The numerical results were compared with experimental measurements. Figure 3 compares the experimental and numerical speed and discharge coefficients at runaway condition for different wicket gate angles. The maximum differences between numerical and experimental speed coefficients were observed at the highest wicket gate angles for each test case. The maximum differences between numerical and experimental speeds are presented in table 3.

The numerical simulation also predicted the discharge coefficients at the runaway speed condition, as shown in figure 3 (left). The numerical values agree well with experimental data, with a maximum difference of 6% and 8.9% for cases 2 and 3 at wicket gate angle of 26°. The discrepancy was 7.5% for case 1 at wicket gate angle of 11.5°. Figure 3 (right) shows the runaway speed lines, computed from numerical and experimental results, for all test cases. In figure 3, the curves A_1, A_2, B_1, B_2, C_1 and C_2 present the runaway speed operating condition, which were obtained for wicket gate angles of 26° in case 1 and 2, and 15° in case 3, respectively. It is clear that runaway lines follow the same trend

for each test case, but a little deviation is observed for higher speed coefficients, for instance, between A_1 and A_2, and between B_1 and B_2.

Table 3. Maximum discrepancy between the numerical and experimental speed coefficients.

Case	Wicket gate opening	Discrepancy
1	22°	5.65 %
2	26°	3.94 %
3	30°	3.80 %

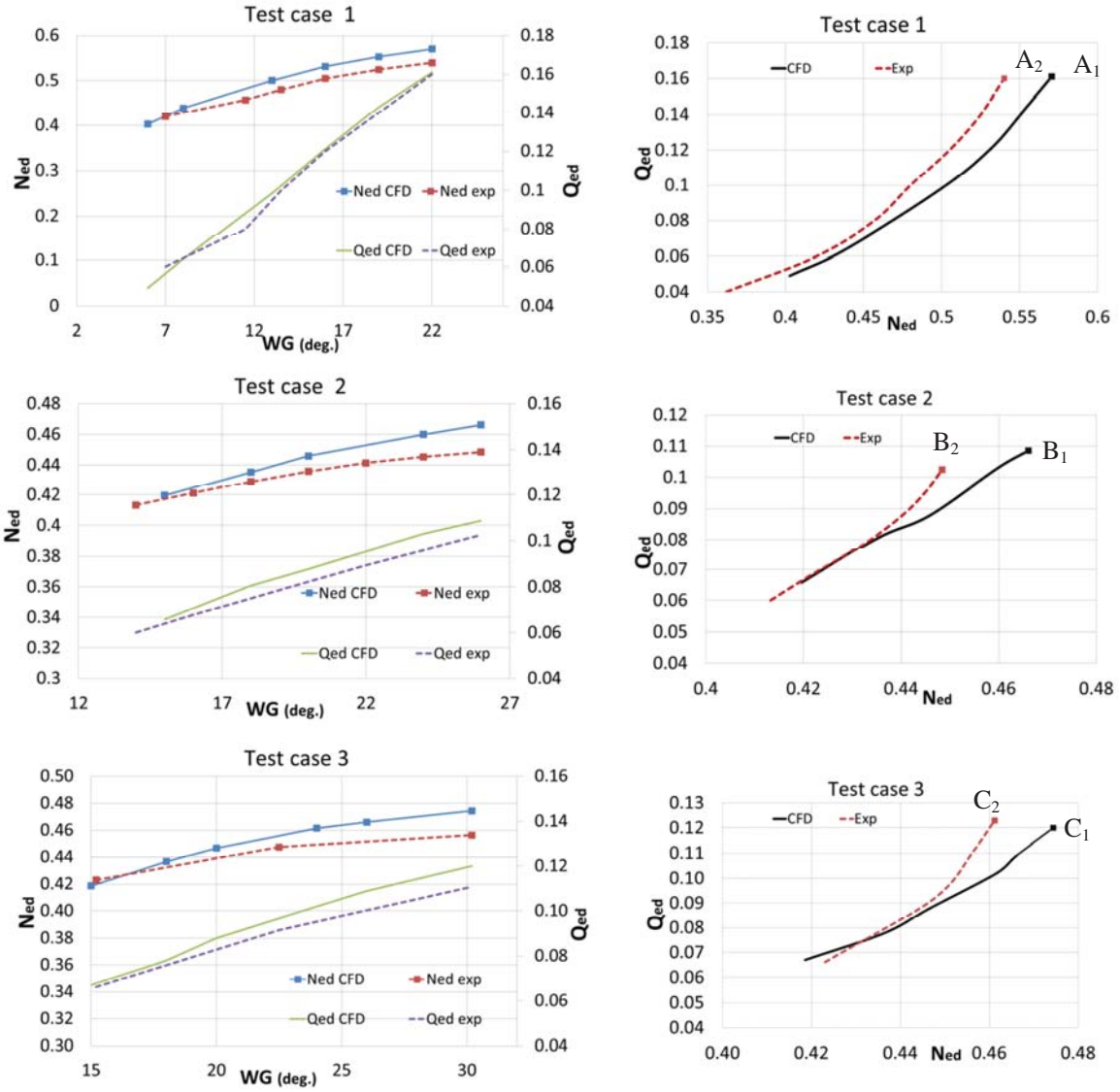

Figure 3. Turbine dimensionless parameter predictions from CFD & experiment at no-load condition.

The discrepancies between numerical and experimental results might be due to steady-state simulations, which could not capture the unsteady flow phenomena such as vortex break down, rotor-stator interaction and vortex shedding inside flow passages. It is expected to obtain more accurate results by performing unsteady simulations in a fluid domain with very fine meshes. However, it

would require an extra computing effort. Overall, from the results, it appears that the runaway speeds were well predicted through the proposed methodology.

According to the proposed methodology, the steady-state computations are performed at operating points that have been specified based on the false position method. The computations are completed when the turbine torque and efficiency become small enough. Figure 4 shows the evolution of the power coefficient P_{ed}, which corresponds to turbine torque and rotational speed as shown in equation (17), for selected operating points. In figure 4 (left), the power coefficient decreases gradually when the speed coefficient increases in runaway speed computations. The points close to the N_{ed}-axis are shown in figure 4 (right). They show that when approaching runaway speed, a large drop of the power coefficient occurs for a small increase of the speed coefficient. For instance, the power coefficient decreases by 335% between E_1 and E_2, while the speed coefficient simultaneously increases by 0.09%, as detailed in table 4.

The sudden power coefficient drop near the horizontal axis shows the existence of a power coefficient threshold. The power coefficient deviation reduced the convergence accuracy for operating points, selected near the drop. In the present study, the results showed that a power coefficient range from -0.01 to 0.01 is suitable for predicting the runaway speed with an adequate level of accuracy.

Table 4. Maximum variation of dimensionless parameters near the N_{ed}-axis.

Wicket gate opening	Points	N_{ed}	P_{ed}
15°	E_1-E_2	0.09 %	-335 %
18°	F_1-F_2	0.16 %	-193 %

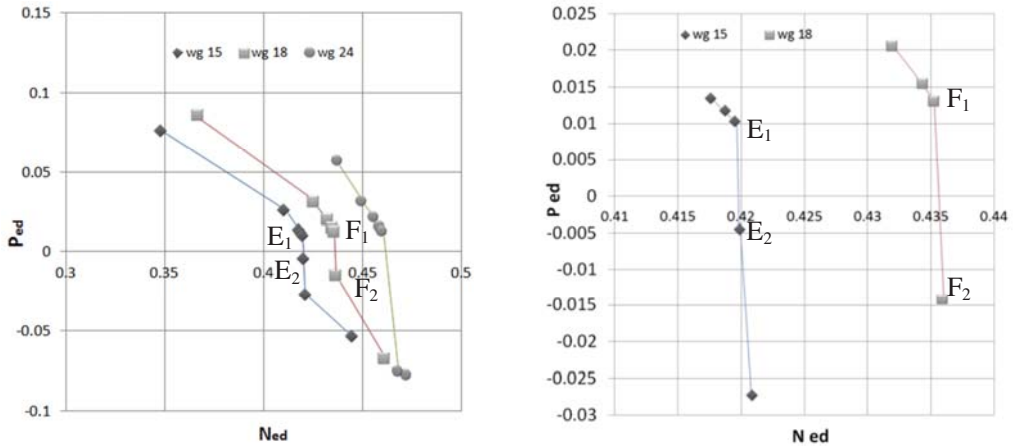

Figure 4. Power factor P_{ed} vs. speed factor N_{ed} for test case 2.

4. Conclusion

In a runner design process, the accurate determination of runaway speed is important to ensure the safe operation of the hydropower plant. Hence this paper presented a CFD method for computing runaway speed of Francis turbine runners at different opening angles. The proposed methodology is robust and economical in terms of computational resources because it uses steady-state stage computations and a simple algorithm based on the smooth relation between torque and speed.

The methodology was assessed by calculating turbine dynamic parameters: speed factor, discharge factor and power factor during runaway speed for three test cases consisting of high and medium head Francis turbines. The speed factor and discharge factor had less than 5.65 % and 8.9 % deviation from the experiments in all tested openings, respectively. The runaway speed line, which was obtained from numerical results, had a trend similar to the experimental one, but there was some deviation from the experimental line for higher opening angles. Overall, the numerical results agreed well with experimental data. The proposed method can be applied by design engineers in order to compute runaway speed in a wide range of operating conditions with an adequate level of accuracy.

References

[1] Nicolet C, Arpe J, and Avellan F, "Identification and Modeling of Pressure Fluctuations of a Francis Turbine Scale Model at Part Load Operation," in *Proceedings of the 22nd IAHR Symposium on Hydraulic Machinery and Systems 2004*.

[2] Ruprecht A, Helmrich T, Aschenbrenner T, and Scherer T, "Simulation Of Vortex Rope In A Turbine Draft Tube " in *the Hydraulic Machinery and Systems 21st IAHR Symposium*, Lausanne 2002.

[3] Levchenya A M, Smirnov E M, and Goryachev V D, "RANS-based numerical simulation and visualization of the horseshoe vortex system in the leading edge endwall region of a symmetric body," *International Journal of Heat and Fluid Flow,* vol. 31, pp. 1107-1112, 2010.

[4] Guo C, Wang G, and Xiao J, "Numerical Simulation for Hydraulic Characteristics of Cylindrical Valve in Runaway Protection Process," in *Power and Energy Engineering Conference,. APPEEC 2009*.

[5] Nennemann B, Vu T C, and Farhat M, "CFD prediction of unsteady wicket gate-runner interaction in Francis turbines: A new standard hydraulic design procedure," presented at the HYDRO 2005 International Conference and Exhibition, Villach, Austria, 2005.

[6] Cherny S et al., "3D numerical simulation of transient processes in hydraulic turbines," *IOP Conference Series: Earth and Environmental Science,* vol. 12, p. 012071, 2010.

[7] Kolšek T, Duhovnik J, and Bergant A, "Simulation of unsteady flow and runner rotation during shut-down of an axial water turbine," *Journal of Hydraulic Research,* vol. 44, pp. 129-137, 2006.

[8] Nicolle J, Morissette J- F, and Giroux A-M, "Transient CFD simulation of a Francis turbine startup," *IOP Conference Series: Earth and Environmental Science,* vol. 15, p. 2012.

[9] Vu T C and Retieb S, "Accuracy assessment of current CFD tools to predict hydraulic turbine efficiency hill chart," in *Proceedings of the 21st IAHR Symposium on Hydraulic Machinery and Systems*, 2002, pp. 193-198.

[10] Vu T C, Devals C, Zhang Y, Nennemann B, and Guibault F, "Steady and unsteady flow computation in an elbow draft tube with experimental validation," in *25th IAHR Symposium on Hydraulic Machinery and Systems, 20-24 Sept. 2010*.

[11] Davidson P A, *Turbulence: an introduction for scientists and engineers*: Oxford University Press, 2004.

[12] Galvan S, Reggio M., andGuibault F., "Assessment study of k-ε turbulence models and near-wall modeling for steady state swirling flow analysis in a draft tube using Fluent," *Engineering Applications of Computational Fluid Mechanics,* 2011.

[13] Schlichting H and Gersten K, *Boundary-Layer Theory*: MacGraw-Hill, 2000.

[14] Bilgen E and Boulos R, "Functional Dependence of Torque Coefficient of Coaxial Cylinders on Gap Width and Reynolds Numbers," *Journal of Fluids Engineering,* vol. 95, pp. 122-126, 1973.